EFFECT OF EXTREME COLD WEATHER TEMPERATURE ON CORRODED AND NON-CORRODED BURIED PIPELINES

Qunfang Hu[1], Md Tanvir Ahmed Faysal*[2] and Zhan Su[3]

[1] *Professor, Tongji University, China, e-mail: huqunf@tongji.edu.cn*
[2] *Postgraduate, Tongji University, China, e-mail: tanvirfaysalid@gmail.com*
[3]*Assistant Professor, Shanghai Institute of Disaster Prevention and Relief, e-mail: 2305219@tongji.edu.cn*

***Corresponding Author**

ABSTRACT

Buried pipelines are intensely used for long-distance transportation of essential resources. However, with the increasing service life, corrosion and extreme cold temperature variation related to climate change can weaken the structural integrity of these pipelines, resulting in pipe failures, which brings great environmental and economic disaster and this is a big concern. The purpose of this research is to unveil the effect of cold temperature variation on both corroded and intact pipes and to understand how the additional thermally induced stress can affect already weakened pipes. Using a 3D numerical model, we first simulated the temperature distribution in the soil around the pipe utilizing field monitoring data collected during December 2023 in Shanghai City in Eastern China. Afterwards, a mechanical soil-pipe model for both corroded and intact pipes was developed, similar to the previous model, using the simulated thermal field as a predefined field throughout the whole model. The effect of thermal fluctuation on different zones of both pipes, along with the weakened zone, was discussed broadly. The results indicated that low-temperature fluctuation of the pipe-soil system added a consistent thermal stress, which is most pronounced in the middle part of the pipe where bending moments are highest. Extreme temperature can impose a near-uniform stress increase of up to 4 Mpa of the service stress in intact pipes. Although corrosion moderates the stress concern at the opposite non-corroded part of the pipe, it does not eliminate the thermally driven amplification of stress. Additionally, the cold wave adds a modest, nearly uniform increase of stress but has a midget effect on the dominant stress peaks controlled by the corrosion defect edge. Furthermore, extreme cooling superposes a modest, nearly uniform increase on the circumferential stress field without significantly altering the dominant edge concentration imposed by the defect geometry.

Keywords: *Cold Temperature, Thermal stress, Buried Pipelines, Corrosion*

1. INTRODUCTION

Buried pipelines are crucial for the transportation of essential resources, such as water and power, which significantly impact daily life. Their reliability ensures the continuous supply of these resources, making them vital for infrastructure and public health(Sun et al., 2023). However, the complex and harsh underground condition gradually erode their structural soundness through corrosion(Aslam et al., 2022; Ossai et al., 2015). Corrosion decreases the optimum metal strength and it is one the frontal mechanism that affect the structural integrity of buried steel pipelines(Wasim & Djukic, 2022). It significantly affects buried pipelines by causing localized pitting, which intensifies stresses under external loadings consequently leading to potential failure(C. Q. Li et al., 2017). Many studies have been conducted in recent times to investigate the failure behavior as well as strength strength-influencing factor of pipeline having wall thinning problems using full scale laboratory testing and finite element analysis. Oh et al conducted seven full-scale laboratory test of corroded pipeline to find out the failure behavior of buried pipelines using stress-based local failure criteria. The specimen had simulated gauge corrosion defect and it was under internal pressure. He found out that the gauge defect with the increase of defect size the ultimate pressure the pipe can withstand, gets substantially reduced(Oh et al., 2007). Another experimental study done by Benjamin et al showed, twelve burst pressure tests on pipeline tubular specimens containing a pipe without defects and the other two had single small base defects of different depths. Nine of the specimens contained interacting corrosion defects, which were composed of the combination of two or more base defects. He proposed a new method that accounts for the thicker space existing in between the defect and it relies on precise geometric information that captures the spatial arrangement of defects visible in the colony's top view (Benjamin et al., 2007). Mondal et al numerically investigated how corrosion defect's orientation at different inclination angles influence pipeline burst pressure, aiming to evaluate the applicability of the ASME B31G guideline. Based on a parametric study, he proposed a predictive model for the burst pressure of pipelines containing inclined corrosion defects(Mondal & Dhar, 2025). Li et al also developed Finite element models of uniformly and non-uniformly corroded steel pipes. The influence of corrosion shape on stress distribution and failure pressure under uniform corrosion conditions was analyzed with introducing a fractal dimension to investigate the effects of surface complexity on failure pressure of pipelines. The analysis shows that steel pipes with elliptical corrosion outperform the rectangular defects in terms of burst capacity, and the difference increases as the defect length increases. Moreover, a more intricate corrosion surface markedly lowers the failure pressure. This trend holds for both defect geometries(P. Li, Li, Fang, Du, et al., 2025; P. Li, Li, Fang, Wang, et al., 2025). Observations from the trend of the research indicate that most of the investigations put emphasis on only corrosion and its parametric influence on the pipeline failure. However, the other external factors that can influence an already weaken pipeline is insufficiently explored. Specifically, studies highlighting the mechanical behavior of the buried pipeline under the cold temperature fluctuation is lacking. Environmental temperature fluctuations have a considerable effect on the integrity of pipelines. It generates thermal stress and mechanical damages. Climate is considered one of the significant factors influencing pipe failure(Żywiec et al., 2021). Older pipes are more vulnerable to such effects as their remaining yield strength is close to the external load(Sadiq et al., 2004). In colder climates, the fracture toughness of pipeline steel decreases and it gets more susceptible to cracking and failure under stress(Chanda, 2015). Temperature fluctuations may cause axial deformation by causing thermal expansion and contraction. It is influenced by the thermomechanical behavior of the pipeline materials, which can lead to stress concentration at these weak points. Pipelines subjected to sinusoidal temperature variations experience local and linearized elastic thermal stresses. These stresses are influenced by the pipe's cross-sectional properties, load frequencies, and heat transfer coefficients (Adolfsson, 2023). Cold temperature can drastically lower the temperatures of air, soil, and the water within buried pipelines, consequently a range of adverse effects such as pipe bursts, water leakage, structural damage, service disruptions, and a shortened operational lifespan of the pipeline infrastructure arise(H. Li et al., 2020). Pipe failure due to cold temperatures is a well-known phenomenon in the existing literature(Hu et al., 2024, 2025). Habibian et al investigated the effect of temperature changes on water-main breaks and highlighted that the break activity is not uniquely related to the temperature. Additionally, he shows how different break

activities may occur under similar temperature-drop conditions(Habibian, 1994). Rajani et al examines the impact of temperature changes on observed pipe breakage rate of different material. The authors found a rise in failure rates associated with rapid temperature fluctuations, with cast iron pipes being the most significantly affected by these changes(Rajani et al., 2012).The findings from the research trend suggest that much of the focus has been on assessing the impact of low temperatures on the failure rate of buried pipes, as well as modelling and predicting pipeline network failures using historical data on climatic factors. In-fact, the mechanical response of pipelines to cold temperature is complex and influenced by several factors. The additional stress generated by cold event induced thermal variation can have much impact on a corroded pipeline which is already weaken by the wall thinning process. In a coupled scenario where the additional stress can reduce the maximum service life of a corroded pipeline which is overlooked by the previous studies. So, it is necessary to investigate how corrosion by reducing the ultimate strength of the pipe material can interact with the added thermal induced mechanical load affect the optimal operational ability of a buried pipeline.

2. METHODOLOGY

In this study a sequentially coupled thermo- mechanical analysis of the soil-pipe model was constructed, because the one-way dependence in which the stress field is governed by the temperature distribution while the temperature field itself can be resolved independently of the mechanical response. The thermal field affects the mechanical field for example, Thermal expansion, but the Mechanical field does not affect the thermal field. The analyses are conventionally executed in sequence, with the thermal simulation completed first and the mechanical stress analysis performed thereafter. The temperatures are read into the stress analysis as a predefined field by reading the output database or the results file from the corresponding heat transfer analysis.

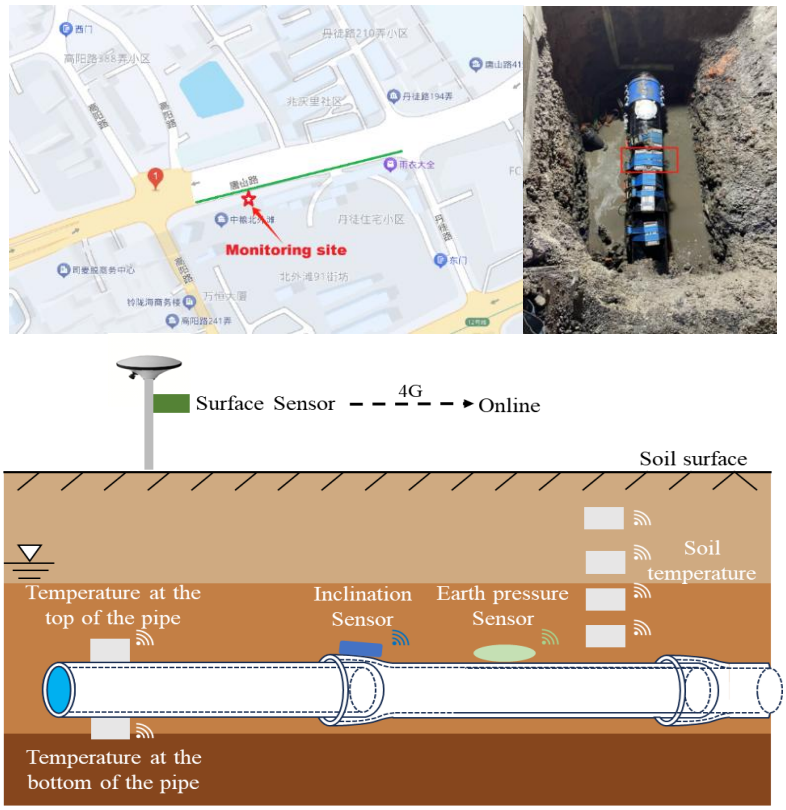

Figure 1: Site location and Positions of various temperature sensors

The temperature varies with position and is usually time-dependent. It is predefined because it is not changed by the stress analysis solution. The element type for the thermal analysis step was the three-

dimensional 8-node linear heat transfer brick element (DC3D8). The element has 8 degrees of freedom, corresponding to temperature values at its 8 modes. For the mechanical analysis, the 8-node brick elements with reduced integration (C3D8R) were utilized.

2.1 Temperature Data Acquisition and Establishment of the Soil-Thermal Model

The monitoring site on buried water distribution pipeline was located Approximately 80 meters east of the intersection of Tangshan Road and Gaoyang Road, on the south side of the road at the Yangpu district of Shanghai, Chin. Yangpu area has hot summer and cold winter which have an average annual maximum and minimum air temperatures of 17.84 ◦C and 6.27 ◦C, respectively. Figure 1. Shows the location and the monitoring site. The soil at the monitoring station and around the buried pipeline is mainly cohesive and sandy soils. The buried pipeline is a water distribution pipeline with nominal diameter of 300 mm. The burial depth of the pipe from the soil surface is 1.1m. For, the temperature monitoring a special 2A0X Type - WiSenMeshWAN @ Multi-channel Soil Temperature Sensor was used which can capture a Standard range of 30°C~ +70°C temperature with an accuracy of ±0.2°C. Figure 1 Shows Positions of various temperature sensors. A three-dimensional finite element model implemented in Abaqus v6.14 was employed to assess the thermal propagation of the soil model due to surface temperature of the soil. So, the simulated soil- pipeline model. The pipeline is buried at a depth of 1.1m below the soil top surface. Based on Saint-Venent's principle, to minimize boundary interference, soil model dimensions should typically be 3 ~ 5 times the pipe diameter(Whidden, 2009). So, the dimensions of the surrounding soil in the FE model were set at about 7.0 m (height) by 6.0 m (width) by 3.0 m (length). The thermal material properties of the soil and pipe used in this study are presented in Table 1.

Table 1: Thermal properties of soil and pipe

Parameters	Pipe	Soil
Density (kg/m3)	7300	1900
Thermal conductivity (W/m℃)	30.3	0.3
Specific heat (J/kg℃)	600	350

The boundary condition for the numerical model was as the soil surface temperature, which includes a maximum and minimum air temperature of 6.6 °C to a maximum of 13.3 °C a span of 19.9 °C within 217 hours period. The initial temperature of this numerical model is set by using a predefined field, as in the actual condition the soil surface remain in contact of environment. So as the initial temperature boundary, top and bottom part of the pipe namely pipe top and bottom part was given an initial temperature of 8.8 °C from the top surface to 1.1 m and from 1.4 to 7m 11.9 °C respectively. An adiabatic boundary condition was considered for surfaces around soil model.

The accuracy of the thermal propagation throughout pipe-soil model is one of the main parts in sequentially thermo-mechanical modelling process. Comparisons of the soil temperature at the top of the pipe are presented in Figure 2. It shows that numerically calculated soil temperature data closely matches with the field monitoring data. It means that in the numerical model, the surface temperature of the soil is propagating through the soil to the buried pipe similar to the actual condition.

2.2 Establishment of the Mechanical model

Using similar numerical model to the previous, one corroded and one non-corroded pipe soil mechanical model was developed to understand the cold event induced stress state of buried pipeline. For this analysis the material property of pipeline and corrosion characteristics has been presented in Table 2. A sufficiently long pipe segment was considered to keep the boundary far from the corrosion zone and thus avoid the boundary effects(Fekete & Varga, 2012). To understand the mechanical behavior of the soil material Mohr-Coulomb constitutive model was used(Coombs et al., 2013; Handspiker et al., 2024).

Table 2: Properties of the pipe and soil used for Mechanical analysis

Parameters	Pipe	Soil
Density (kg/m3)	7300	1900
Modulus of elasticity, E(GPa)	210.7	20
Poisson's ratio	0.30	0.35
Yield strength, σy (MPa)	464.5	--
Ultimate tensile strength, σu (MPa)	563.8	--
Thermal expansion	1.2×10^{-5}	10^{-4}
Cohesion, c (kPa)	--	5
Friction angle (◦)	--	35
Dilation angle (◦)	--	3.5
Pipe diameter, D (mm)	762	--
Wall thickness, t (mm)	17.5	--
Corrosion length, l (mm)	200	--
Corrosion width, c (mm)	50	--
Corrosion depth, d (mm)	8.75	--

The soil was assumed to be an isotropic material, having the same characteristic throughout the whole volume in different temperature. Surface to surface contact was used on the soil pipe model with using hard contact in norma direction and penalty with a friction coefficient of 0.2 in tangential direction. The pipeline was used as an elastic plastic material. In this analysis the most bottom surface of the soil was constrained from all three(X,Y,Z=0) direction with respect to displacement.

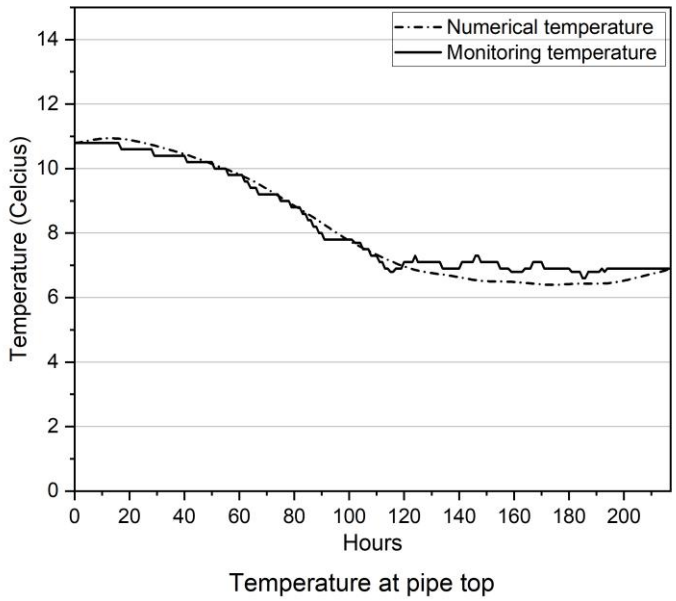

Figure 2: Comparison of numerical result with field temperature data at the top

The both side surface of the soil was restrained in X direction, Similarly the soil surface was also restrained in Z direction with respect to direction. The soil top surface was left unconstrained and taken as a free surface. All loading was set up by four steps. In the first step the whole model was subjected to gravity load. Then in the second step the pipelines internal wall was given an internal operational pressure of 0.2 MPa which is very common in water pipeline. In the third step traffic loading was introduced. Since most of the water pipelines re being buried under roads, self-weight of the vehicle directly influences on the pipeline through the pavement of the road.

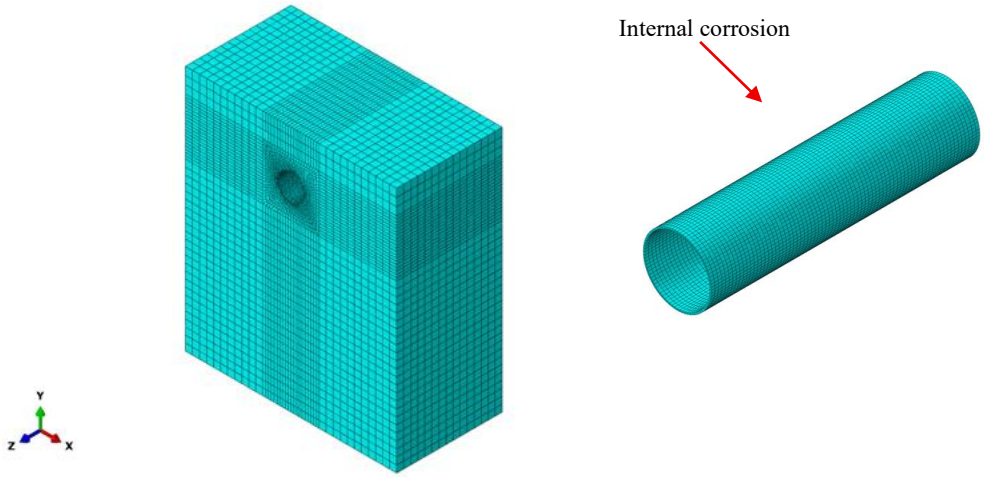

Figure 3: Soil and pipe models

To simplify the analysis a static traffic load was taken as a static load. It is a common phenomenon and its suitability to adequately represent traffic loading has been established (Alzabeebee et al., 2018). In this analysis, a static load of 0.7 MPa was applied to the top surface of the model and at the top of the corrosion as this is the most vulnerable zone of a corroded pipe. Finally, in the fourth step thermal analysis result was used as the predefined field. Traditional stress-based design (Von Mises) criterion is used for the mechanical analysis as it accounts for the effects of all the principal stresses (Gong et al., 2024).

3. RESULTS AND DISCUSSION

3.1 Analysis of Stress distribution in intact zone

The stress analysis of both the corroded and non-corroded pipe due to cold temperature fluctuations was explored by studying the Von Mises stress along the pipe axis. Stress distributions in longitudinal direction at the top and bottom part of the interior surface around the corrode zone and in circumferential direction at the middle and edges of corrosion were studied to uphold a comprehensive understanding of the response of thermal stress to a corroded and non-corroded buried pipe. Figure 4. Shows the distribution of Von Mises stress of a non-corroded pipe at the top inner surface of the pipe along the longitudinal direction. The figure depicts the longitudinal distribution of Von Mises stress along the non-corroded pipe top under identical loading before and after the cold temperature event. In both cases, the stress profile was similar, reaching its maximum at the mid-span and tapering toward the ends, a pattern characteristic of bending-dominated behavior. Prior to the cold event, the peak stress attains 19 MPa, whereas post-event stress raised to 21 MPa, an increase of roughly 10 %, which is consistent with previous numerical studies showing that cold waves can elevate Von Mises stress in buried pipelines by roughly 10–20 % depending on loading and burial conditions(Hu, Ayinde, et al., 2024; Shishesaz et al., 2024). A similar stress increase can also be observed at the inlets and outlets, where stresses climb from about 14.5 MPa to 16.5 MPa. The upward translation of stress indicates that exposure to low temperature fluctuations adds consistent thermally induced stresses, which is likely caused by contraction of the pipe and surrounding soil. Consequently, the cold wave amplifies Von Mises stresses along the entire top.

Figure 5. summarizes the Von Mises stress, along the bottom of the 3 m long pipeline of four thermo-mechanical states at the pipe bottom. For the non-corroded pipe, the cold wave produces an almost rigid stress rise on the whole body. In the mid-span stress jumps from about 14.8 MPa to 18.0 MPa containing 21.6 % hike, while the stress at both ends of the pipe rises from 12.0 MPa to

15.5 MPa containing 29 %. This uniform uplift reflects similar behavior to the top of the pipe. However, the magnitude of the stress is higher at the top compared to the bottom of the non-corroded pipe. This observation aligns directly with (Ma et al., 2024)who conducted a comprehensive finite element analysis of X80 steel pipelines with corrosion defects and explicitly found that "stress at the bottom of the pipe is less than that at the top," with stress at the top of the pipeline being greater than the bottom across multiple loading scenarios.

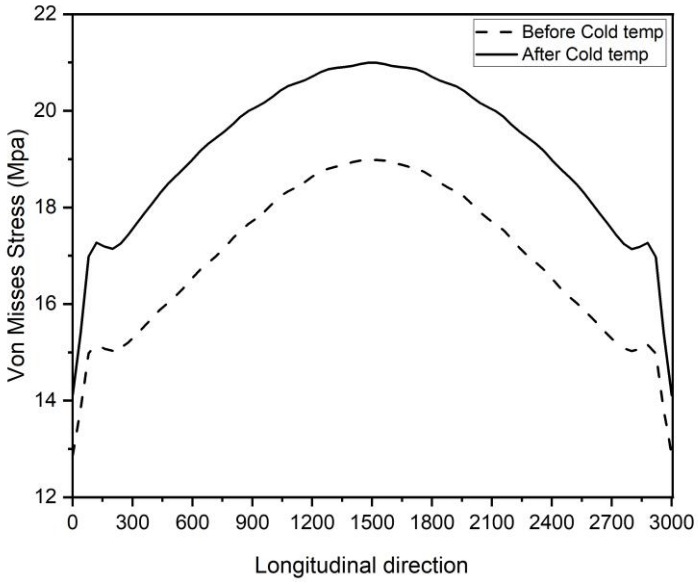

Figure 4: Stress distribution of a non-corroded pipe before and after cold temp at the pipe top

In the corroded pipe, wall-thinning lowers the absolute stress field at the bottom of the pipe by about 2.5 MPa because the reduced wall thickness at the top allows greater concentration of stress at the corroded zone.

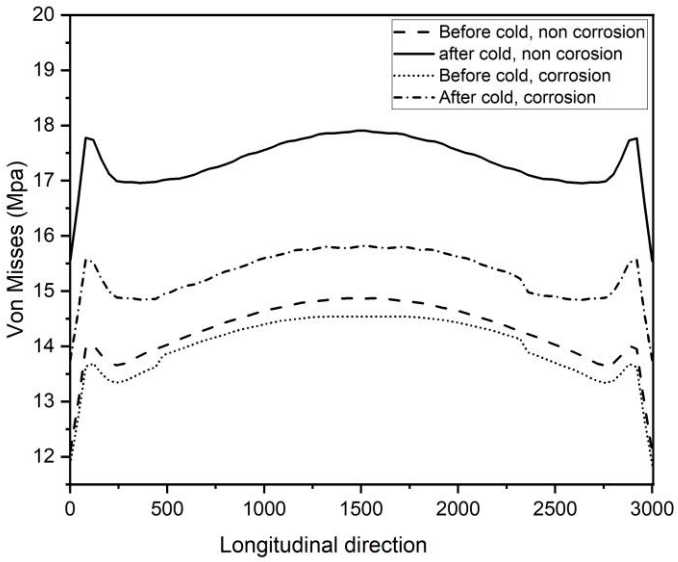

Figure 5: Stress distribution of both pipe before and after cold temp at pipe bottom

Nonetheless, the temperature effect remains pronounced. After the cold temp, at mid-span, stress increases from about 14.5 MPa to 15.8 MPa and the end stresses rise from 12 MPa to 14 MPa. which is similar to the findings by (Cheng et al., 2022)that corrosion defects redirect stress concentration to thinned regions while maintaining thermal sensitivity across the pipe cross-section.

3.2 Analysis of Stress distribution in corroded zone

Figure 6. displays the longitudinal distribution of Von Mises equivalent stress, of a pipeline containing a centrally located corrosion defect which is subjected to identical loading conditions. Outside the defective zone (0-1.40 m and 1.6–3.00 m) the stress response is almost similar from around 12.5 MPa at the restrained ends to 20 MPa adjacent to the defect. Following the temperature drop stress in the non-corroded zone is increased by 1-1.5 MPa which is about 7-9 %, reflecting the additional stress imparted by the thermal stress.

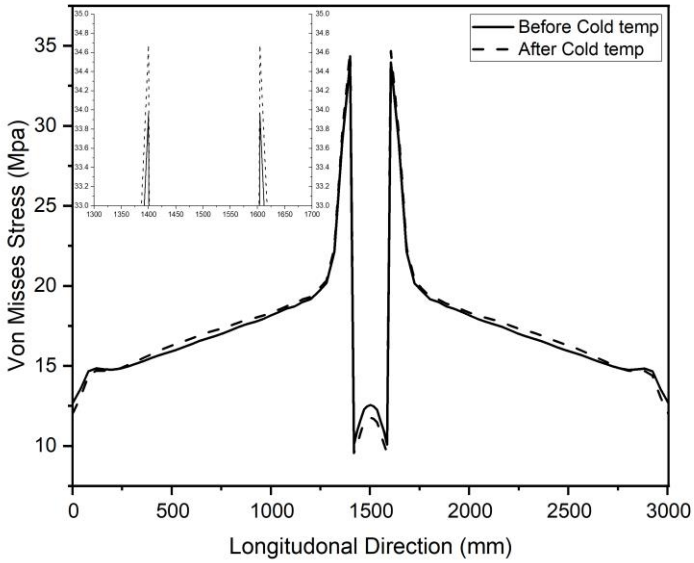

Figure 6: Stress distribution of the Corroded pipe before and after cold temp at corrosion zone

Within the defect itself 1.4-1.60 m the stress field is dominated by geometric discontinuities. It can be seen, stress at the corrosion edge is 34 MPa in the pre-cooling state and increases slightly to 34.8 MPa post-cooling, which is about 1.5 % increase in stress threshold. Between these edges the thinned wall carries markedly lower stress, dipping to 14 MPa before the cold wave and to 11 MPa afterwards which may yield because of a substantial stress concentration around the corrosion edge. Thus, while the cold wave event superimposes a nearly uniform thermal hike over the pipe length, it has only a marginal influence on the already dominant stress concentration at the defect edges. The results suggest that, for corroded pipelines, peak stresses are controlled primarily by defect geometry, with extremely low temperature acting as a secondary amplifying factor.

Figure 7 presents the circumferential distribution of Von Mises equivalent stress, for a pipe section containing an internal corrosion defect, immediately before and after a pronounced cold event at two axial locations which are the center of the defect and its longitudinal edge. The consecutive finite-element numbers around the pipe wall; zero corresponds to the bottom and the sequence proceeds clockwise until it comes back to zero. Outside the defect zone the stress field exhibits the characteristic six lobed bending pattern, with a maximum of 14.8 MPa prior to cooling. Thermal stress elevates stress uniformly by 1 MPa which is around 7 % increase at the bottom. However, the center of the circumferential edge carries lower load, and peaks at only about 11 MPa before cooling. After post-cooling stress is marginally reduced to 10 MPa, indicating that the thermal contraction has redistributed load from the weakened mid defect strip toward it's the edge.

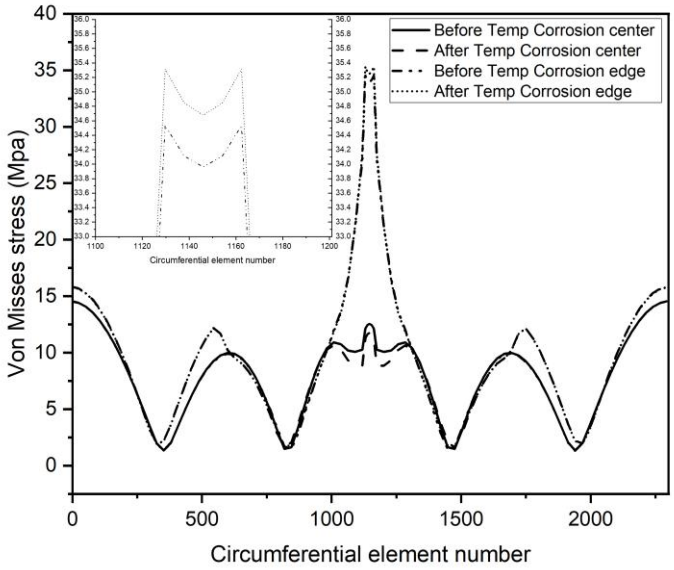

Figure 7: Stress distribution of the Corroded pipe before and after cold temp at corrosion zone

In contrast, the defect edge from a sharp geometric discontinuity concentrates stress. it reaches 34.3 MPa in the pre-cooling state and rises to 35.3 MPa after the cold temperature event, which is an increment of 1 MPa or 3 %. The inset enlarges this region, highlighting that the thermal fluctuation simply adds to the existing concentration without altering its spatial extent.

4. CONCLUSIONS

A comprehensive thermo-mechanical assessment of a buried concrete pipeline was performed to quantify how short-term cold temperature excursions interact with traffic loading and corrosion morphology to influence Von Mises stress.

1. Cold weather temperature adds a consistent thermal stress throughout the whole pipe. This is likely caused by the continuous contraction of the pipe and the surrounding soil.
2. Extreme cold temperature can impose a near-uniform stress leap up to 4 MPa on the service stress in intact pipes. Secondly, although corrosion moderates the stress concentration at the opposite part of the pipe, it does not eliminate the thermally driven amplification of Stress.
3. In the corroded pipe thermal stress is very low in non-corroded areas. However, at the corroded zone the effect of cold temperature is higher. Furthermore, additional stress tends to accumulate at the Corrosion edges rather than the rest of the surface of the pipe because of the stress concentration.
4. Cold weather temperature generates a modest, nearly uniform increase of stress on the circumferential direction without significantly altering the dominant edge concentration imposed by the defect geometry.

ACKNOWLEDGEMENTS

This study was funded by the National Key Research and Development Program of China (2024YFC3808600, 2022YFC3801000), Natural Science Foundation of Shanghai (24ZR1470300) and Shanghai Chengtou Water Group Co. Research Project (KY.WB.23.012).

DECLARATION OF USE OF AI

AI tools were employed to review and improve the clarity, grammar, and overall presentation of the manuscript text. All AI-generated suggestions were reviewed and approved by the authors prior to inclusion.

REFERENCES

Adolfsson, E. (2023). Stresses in pipes subject to thermal fluctuations and linear temperature ramps. *International Journal of Pressure Vessels and Piping*, *206*, 105055. https://doi.org/10.1016/j.ijpvp.2023.105055

Alzabeebee, S., Chapman, D. N., & Faramarzi, A. (2018). A comparative study of the response of buried pipes under static and moving loads. *Transportation Geotechnics*, *15*, 39–46. https://doi.org/10.1016/j.trgeo.2018.03.001

Aslam, R., Mobin, M., Zehra, S., & Aslam, J. (2022). A comprehensive review of corrosion inhibitors employed to mitigate stainless steel corrosion in different environments. *Journal of Molecular Liquids*, *364*, 119992. https://doi.org/10.1016/j.molliq.2022.119992

Benjamin, A. C., Freire, J. L. F., & Vieira, R. D. (2007). PART 6: ANALYSIS OF PIPELINE CONTAINING INTERACTING CORROSION DEFECTS. *Experimental Techniques*, *31*(3), 74–82. https://doi.org/10.1111/j.1747-1567.2007.00190.x

Chanda, S. (2015). *Temperature effects on dynamic fracture of pipeline steel* [University of Alberta Library]. https://doi.org/10.7939/R3695Q

Cheng, Y., Liu, P., & Yang, M. (2022). Effects of Temperature and Applied Potential on the Stress Corrosion Cracking of X80 Steel in a Xinzhou Simulated Soil Solution. *Materials*, *15*(7), 2560. https://doi.org/10.3390/ma15072560

Coombs, W. M., Crouch, R. S., & Heaney, C. E. (2013). Observations on Mohr-Coulomb Plasticity under Plane Strain. *Journal of Engineering Mechanics*, *139*(9), 1218–1228. https://doi.org/10.1061/(ASCE)EM.1943-7889.0000568

Fekete, G., & Varga, L. (2012). The effect of the width to length ratios of corrosion defects on the burst pressures of transmission pipelines. *Engineering Failure Analysis*, *21*, 21–30. https://doi.org/10.1016/j.engfailanal.2011.12.002

Gong, C., Guo, S., Zhang, R., & Frangopol, D. M. (2024). Prediction of burst pressure of corroded thin-walled pipeline elbows subjected to internal pressure. *Thin-Walled Structures*, *199*, 111861. https://doi.org/10.1016/j.tws.2024.111861

Habibian, A. (1994). Effect of Temperature Changes on Water-Main Breaks. *Journal of Transportation Engineering*, *120*(2), 312–321. https://doi.org/10.1061/(ASCE)0733-947X(1994)120:2(312)

Handspiker, W., Liu, Z., & Ghafghazi, M. (2024). On stress ratio equations in three-dimensional stress space for modelling soil behaviour. *Geotechnical Research*, *11*(4), 243–255. https://doi.org/10.1680/jgere.23.00073

Hu, Q., Ayinde, O., & Liu, W. (2024). Mechanical response of buried water pipes to traffic loading before and after extreme cold waves. *Transportation Geotechnics*, *49*, 101418. https://doi.org/10.1016/j.trgeo.2024.101418

Hu, Q., Che, D., Wang, F., & He, L. (2024). Analyzing the effects of extreme cold waves on urban water supply network safety: A case study from 2020 to 2021. *Urban Climate*, *58*, 102146. https://doi.org/10.1016/j.uclim.2024.102146

Hu, Q., Che, D., Zhang, Q., Zhou, J., Wang, F., Zhang, Z., & Song, Z. (2025). Improving underground pipeline resilience: Prediction and interpretability analysis of urban water

distribution network pipe failures during cold waves using machine learning. *Tunnelling and Underground Space Technology*, *163*, 106717. https://doi.org/10.1016/j.tust.2025.106717

Li, C. Q., Wang, W., Robert, D., & Zhou, A. (2017). *Investigation of corrosion effect on underground metal pipes*. 1–11.

Li, H., Lai, Y., & Li, L. (2020). Impact of hydro-thermal behaviour around a buried pipeline in cold regions. *Cold Regions Science and Technology*, *171*, 102961. https://doi.org/10.1016/j.coldregions.2019.102961

Li, P., Li, B., Fang, H., Du, X., Wang, N., Zang, Q., & Di, D. (2025). 3D fractal modeling of non-uniform corrosion in steel pipes: Failure behavior analysis and structural integrity assessment. *Reliability Engineering & System Safety*, *261*, 111111. https://doi.org/10.1016/j.ress.2025.111111

Li, P., Li, B., Fang, H., Wang, N., Di, D., Du, X., Li, M., & Zhai, K. (2025). 3D fractal modeling of corrosion defects: Failure pressure prediction for steel pipes integrating defect geometry and fractal surface features. *Engineering Failure Analysis*, *178*, 109744. https://doi.org/10.1016/j.engfailanal.2025.109744

Ma, Y., Li, B., Fang, H., Du, X., Wang, N., Zhai, K., & Di, D. (2024). *The Longitudinal Mechanical Behavior of Steel Pipes with Pitting Corrosion Under the Coupling Effect of Complex Service Loads*. SSRN. https://doi.org/10.2139/ssrn.4935241

Mondal, B. C., & Dhar, A. S. (2025). Investigation of the Burst Pressure of a Pipeline with an Inclined Corrosion Defect Using FE Analysis. *Journal of Pipeline Systems Engineering and Practice*, *16*(2), 04025015. https://doi.org/10.1061/JPSEA2.PSENG-1803

Oh, C.-K., Kim, Y.-J., Baek, J.-H., Kim, Y.-P., & Kim, W.-S. (2007). Ductile failure analysis of API X65 pipes with notch-type defects using a local fracture criterion. *International Journal of Pressure Vessels and Piping*, *84*(8), 512–525. https://doi.org/10.1016/j.ijpvp.2007.03.002

Ossai, C. I., Boswell, B., & Davies, I. J. (2015). Pipeline failures in corrosive environments – A conceptual analysis of trends and effects. *Engineering Failure Analysis*, *53*, 36–58. https://doi.org/10.1016/j.engfailanal.2015.03.004

Rajani, B., Kleiner, Y., & Sink, J.-E. (2012). Exploration of the relationship between water main breaks and temperature covariates. *Urban Water Journal*, *9*(2), 67–84. https://doi.org/10.1080/1573062X.2011.630093

Sadiq, R., Rajani, B., & Kleiner, Y. (2004). Probabilistic risk analysis of corrosion associated failures in cast iron water mains. *Reliability Engineering & System Safety*, *86*(1), 1–10. https://doi.org/10.1016/j.ress.2003.12.007

Shishesaz, M., Gatea, A. H., Moradi, S., & Yaghoubi, S. (2024). Stress analysis in the buried polyethylene pipes with viscoelastic behavior: A finite element study. *Discover Applied Sciences*, *6*(11), 616. https://doi.org/10.1007/s42452-024-06331-0

Sun, Y., Ren, Y., & Cheng, Y. F. (2023). Dissociative adsorption of hydrogen at edge dislocation emergence on α-Fe studied by density functional theory. *International Journal of Hydrogen Energy*, *48*(98), 38821–38841. https://doi.org/10.1016/j.ijhydene.2023.06.198

Wasim, M., & Djukic, M. B. (2022). External corrosion of oil and gas pipelines: A review of failure mechanisms and predictive preventions. *Journal of Natural Gas Science and Engineering*, *100*, 104467. https://doi.org/10.1016/j.jngse.2022.104467

Whidden, W. R. (Ed.). (2009). *Buried Flexible Steel Pipe: Design and Structural Analysis*. American Society of Civil Engineers. https://doi.org/10.1061/9780784410585

Żywiec, J., Boryczko, K., & Kowalski, D. (2021). Analysis of the Negative Daily Temperatures Influence on the Failure Rate of the Water Supply Network. *Resources*, *10*(9), 89. https://doi.org/10.3390/resources10090089